Targeting P-selectin and interleukin-1β in mice with sickle cell disease: effects on vaso-occlusion, liver injury and organ iron deposition

Erica M. F. Gotardo,[1] Lidiane S. Torres,[1,2] Bruna Cunha Zaidan,[3] Lucas F. S. Gushiken,[1] Pamela L. Brito,[1] Flavia C. Leonardo,[1] Claudia H. Pellizzon,[4] John Millholland,[5°] Sergei Agoulnik,[6] Jiri Kovarik,[7] Fernando F. Costa[1] and Nicola Conran[1]

[1]Hematology Center, University of Campinas - UNICAMP, Campinas - São Paulo, Brazil; [2]Ruth L. and David S. Gottesman Institute for Stem Cell and Regenerative Medicine Research, Albert Einstein College of Medicine, Bronx, New York, NY, USA; [3]Federal University of Triângulo Mineiro, UFTM, Minas Gerais, Brazil; [4]São Paulo State University (UNESP), Institute of Biosciences, Botucatu, Brazil; [5]Novartis Precision Medicine, Cambridge, MA, USA; [6]Novartis Precision Medicine, Cambridge, MA, USA (former affiliation) and [7]Novartis Biomedical Research, Novartis Campus, Basel, Switzerland

°Current address: Bristol Myers Squibb, Cambridge, MA, USA

Correspondence: N. Conran
conran@unicamp.br

Received: August 14, 2024.
Accepted: November 7, 2024.
Early view: November 21, 2024.

https://doi.org/10.3324/haematol.2024.286418

Supplementary Material

Neutralizing P-selectin and interleukin-1β in mice with sickle cell disease: effects on vaso-occlusive processes and organ injury.

Érica M. F. Gotardo, Lidiane S. Torres, Bruna Cunha Zaidan, Lucas F. S. Gushiken, Pâmela L. Brito, Flavia C. Leonardo, Claudia H. Pellizzon, Sergei Agoulnik, Jiri Kovarik, John Millholland, Fernando F. Costa and Nicola Conran

Supplementary Methods

Animals

Male homozygous Townes mice (*B6;129-Hbb$^{tm2(HBG1,HBB*)Tow}$/Hbb$^{tm3(HBG1,HBB)Tow}$ Hba$^{tm1(HBA)Tow}$/J*) and male Berkeley mice (*Hba^{tm1Paz}Hbb^{tm1Tow}Tg(HBA-HBBs*) 41Paz/J) were used in the study.[1,2] Townes mice were used for acute studies to evaluate microvascular vaso-occlusion, based on previous data from our own studies and those of other authors indicating the suitability of this model,[3,4] and the reliability of our breeding supply. For prolonged studies, we used the Berkeley mouse strain, due to literature reports available at the time of study design describing progressive organ damage similar to that of human SCD.[5] Additionally, our preliminary data from this model enabled us to define a suitable starting time of 16 weeks for antibody administration to capture this damage. Mice were bred from breeders purchased originally from The Jackson Laboratories (Maine, EUA) that were maintained by the animal facility (CEMIB) of the University of Campinas. For some analyses, aged-matched hemizygous littermate mice of the Berkeley strain and age-matched C57BL/7J mice were used as controls. After weaning, mice were maintained at Hematology Center Animal House in microisolators until euthanasia, with food and water *ad libitum*.

Treatment Protocols

Acute protocol (see Figure 1A): Eighteen-week old Townes SCD mice received (i.p.) either saline, or anti-murine IL-1β monoclonal antibody (mAb) (01BSUR IgG2a; 200μg/mouse), and/or anti-murine CD62P (RB40.34 IgG1; 30 μg/mouse), or a control IgG1 antibody (A110-1, 30 μg/mouse), before recombinant murine TNF-α (0.5 μg, *i.p.*, R&D Systems, Minnesota, USA) administration to induce VO processes. Analysis of vaso-occlusion and of blood samples was conducted at 3

hours after TNF-α administration. Anti-murine IL-1β or saline were administered at 24 hours before analyses (i.e., 21 hours before TNF-α). Anti-murine CD62P or control IgG1 were administered at 3.5 hours before analyses (i.e., 0.5 hours before TNF-α). These administration times were chosen based on prior studies of the acute administration of each antibody in inflamed murine models of SCD.[6,7] The mechanistic effects of RB40.34 (anti-P-selectin) IgG1 were compared with those of a control IgG1, due to the non-specific effects of this antibody isotype *in vivo*.[8] Conversely, in mice, the IgG2a isotype causes less non-specific immune interference, compared to IgG1.[9] Therefore, the effects of 01BSUR administration were compared to those of saline. Additionally, the effects of the combined antibody administration were compared to those of control IgG1.

Chronic protocol (see Figure 3A): Sixteen-week old Berkeley SCD mice received (i.p.) anti-IL-1β mAb (7.5 mg/Kg; 2x/week), and/or anti-murine CD62P (30 μg/mouse; 3x/week), or an IgG1 mAb (30 μg/mouse; 3x/week) or saline (2x/week) for 6 weeks. At the end of the treatment, and at 48 hours after the last administration of antibodies, the animals were euthanized and their biological materials collected or analyses carried out. Antibody dosing protocols were used to determine the optimal mAb concentrations and frequencies of administration. Optimal dose concentrations and frequencies of prolonged administration were determined using standardizing protocols, namely maintenance of the inhibition of neutrophil-platelet ($CD45^+Ly6G^+CD41^+$) aggregate formation or reduction of serum IL-6 for 2 weeks (for anti-P-selectin or anti-Il-1β, respectively).

Laser Doppler flowmetry

After anesthesia and trichotomy, laser Doppler flowmetry of the skin microcirculation of the pelvic region of immobilized animals was conducted using the PeriFlux6000 equipment (Perimed, Sweden), employing a 780 nm wavelength laser and the 407 probe. Blood perfusion (in perfusion units) in the pelvic skin microcirculation, within a 10-minute period, was calculated from the mean red blood cell concentration and mean red cell flow velocity (velocity units) using the PeriFlux Configuration Software (PCS). Measurements were normalized relative to each animal's baseline blood perfusion and velocity recorded 48 h earlier.

Intravital Microscopy

Mice were anesthetized at 3-h post TNF-α administration by *i.p.* injection of a ketamine 100 mg/kg + xylazine 10 mg/kg mixture in saline. For the surgical procedure, the animal's cremaster muscle was exteriorized, and stretched over a transparent platform, and continuously irrigated with Ringer's solution (pH 7.4, 37°C). Microvessels (5-9 for each mouse) of 25-35 μm in diameter were visualized using an Axio Imager D2 (Carl Zeiss Microscopy, Jena, Germany; 63X water

immersion objective) that was custom-designed for intravital microscopy. Images from vessels were recorded for 30-60 seconds (40 frames/sec) using an Axiocam 506 color camera (Carl Zeiss Microscopy) and the Zen 2 Pro software (Carl Zeiss Microscopy). The rolling, adhesion and extravasation of leukocytes were quantified according to Almeida et al. (2015).[10] Imaging was performed for a maximum period of 45 min after surgery.

Neutrophil-platelet aggregate analysis by flow cytometry.

Briefly, 50 µl of blood were collected from the retro-orbital plexus with a heparinized capillary. Blood was then incubated with a mix of antibodies in Hank's buffer: PerCP anti-mouse CD45 (30-F11, BioLegend, San Diego, CA, USA), APC anti-mouse Ly6G (1A8, BioLegend) and PE anti-mouse CD41 (MWReg30, BD Biosciences). The samples were stained for 30 min in the dark, at room temperature (RT). After labeling, lysis buffer (1 x Lysing Buffer, BD Biosciences) was added and cells were incubated for 15 min in the dark (RT). After centrifugation (200 *g*, 5 min, RT) and washing, the cell pellets were resuspended in PBS/BSA buffer and data acquisition (50,000 events) was performed on a FACSCalibur™ Flow Cytometer (BD Biosciences). Representative dot plots and analysis of the aggregates are shown in Supplementary Figure 1.

Inflammatory and biochemical marker quantification

IL-1β, tumor necrosis factor (TNF)-α, Interferon (INF)-γ, soluble adhesion molecule intercellular adhesion molecule (sICAM)-1 and IL-6 were measured in serum samples using commercial ELISA kits (IL-1β [high-sensitivity], TNF-α [high-sensitivity], INF-γ, sICAM-1; R&D Systems, Minneapolis, MN, USA. IL-6 [high-sensitivity]; Invitrogen, Vienna, Austria), according to the manufacturers' instructions. Aspartate aminotransferase (ALT) and Alanine aminotransferase (AST) liver enzymes and bilirubin (total, direct and indirect) were quantified in serum, while creatinine was quantified in urine collected on the day of euthanasia, using commercial colorimetric tests (Bioclin, Belo Horizonte, MG, Brazil).

Organ processing and histological staining

Organ specimens were dissected, fixed in 10% formalin solution, and dehydrated in an ethanol sequence before embedding in paraffin. Five-µm sections were stained for histology using hematoxylin-eosin or Masson's trichrome. For evaluating hemosiderin accumulation, sections were incubated with potassium ferrocyanide and hydrochloric acid aqueous solution (1:1 ratio), counterstained with Nuclear Fast Red, and the Prussian blue reaction observed. Areas of sections stained with Prussian blue or Masson's trichome were calculated using Image J analysis software (10 fields/section). The histological analysis of 2-4 sections from each organ was performed blinded by a pathologist, and alterations were scored per organ qualitatively on a scale of 0 (absent), 1 (mild), 2 (moderate) and 3 (severe). Another pathologist carried out a

blinded morphometric analysis on liver sections (2 sections/ organ), counting the number of vessels with at least one red blood cell inside. Histopathological scores for hepatic degeneration, necrosis, renal RBC sickling, alveolar congestion, and pulmonary septal thickening represent the means and SEM of the comprehensive evaluations for each organ assessed; other parameters are depicted as means and SEM of parameter observations from two to three sections or regions of interest per organ evaluated.

lmmunohistochemical Staining

Immunohistochemical staining was performed on paraffin-embedded tissues. Following deparaffinization and rehydration, slides were subjected to heat-mediated antigen retrieval with Tris-EDTA buffer (pH 9.0) in a microwave. After incubating with 30% H_20_2 for 30 min at RT to block endogenous peroxidase activity, slides were incubated overnight with rabbit anti-murine CD68 IgG (EPR23917-164; Abcam, Cambridge, UK) at 4°C. After washing, primary antibody binding was detected using a Rabbit-specific horseradish peroxidase/ 3,3'-Diaminobenzidine detection immunohistochemistry kit (Abcam), according to the manufacturer's instructions. The slides were counterstained with hematoxylin and the percentages of positive-staining cells were calculated using Image J analysis software (10 fields/section).

Quantitative PCR (qPCR)

Organs, dissected at the time of euthanasia, were snap-frozen in liquid nitrogen and stored at -80°C until assay. mRNA was extracted from entire organs using Trizol (Invitrogen, Carlsbad, CA, USA) and a reverse transcription kit was used to synthesize cDNA (RevertAid H Minus First Strand cDNA Synthesis, Thermo Scientific, Waltham, MA, USA). Oligonucleotide primers were designed (Primer-Express; Applied Biosystems, Foster City, CA, USA) to amplify cDNA for conserved regions of the genes encoding proteins of interest (for genes of interest and primer sequences, see Supplementary Table 1); primers were synthesized by IDT (Coralville, Iowa, USA). All samples were assayed in a 12-µL volume containing 10 ng cDNA, 6 µL SYBR Green Master Mix PCR (Applied Biosystems) and gene primers, using a StepOne Real Time PCR System (Applied Biosystems). To confirm the accuracy and reproducibility of the real-time PCR, the intra-assay precision was calculated according to the equation: E(−1 / slope). A dissociation protocol was performed after each run to check for non-specific amplification. Two replicas were run on the plate for each sample. Results are expressed as arbitrary units (A.U.) of gene expression, normalized according to the expressions of Actb and Gpdh through the geNorm program.[11]

Statistical Analysis

Data are expressed as means and standard error of N samples. For comparisons between two groups, the Mann-Whitney test was used. For comparisons between three groups or more, data normality was evaluated. Subsequently, either a One-Way Analysis of Variance (ANOVA) test followed by Dunn's multiple-comparison test (for non-parametric samples) or Holm's-Sidak's multiple comparison test (for parametric samples) was employed. A p value ≤0.05 was considered statistically significant.

Supplementary References.

1. Wu LC, Sun CW, Ryan TM, Pawlik KM, Ren J, Townes TM. Correction of sickle cell disease by homologous recombination in embryonic stem cells. Blood. 2006;108(4):1183-8.
2. Paszty C, Brion CM, Manci E, Witkowska HE, Stevens ME, Mohandas N, et al. Transgenic knockout mice with exclusively human sickle hemoglobin and sickle cell disease. Science. 1997;278(5339):876-8.
3. Jasuja R, Suidan G, Hett SP, Desai K, Le KX, Parks E, et al. Rivipansel: A Small Pan-Selectin Antagonist Improves Cerebral Perfusion and Inhibits Leukocyte Adhesion and in Murine Sickle Cell Disease Model. Blood. 2016;128(22).
4. Torres LS, Gotardo EM, Leonardo FC, Brito PL, Förster I, Kovarik J, et al. Neutralization of Inflammasome-Processed Cytokines Reduces Inflammatory Mechanisms and Leukocyte Recruitment in the Vasculature of TNF-α-Stimulated Sickle Cell Disease Mice. Blood. 2021;138.
5. Manci EA, Hillery CA, Bodian CA, Zhang ZG, Lutty GA, Coller BS. Pathology of Berkeley sickle cell mice: similarities and differences with human sickle cell disease. Blood. 2006;107(4):1651-8.
6. Ghosh S, Flage B, Weidert F, Ofori-Acquah SF. P-selectin plays a role in haem-induced acute lung injury in sickle mice. British Journal of Haematology. 2019;186(2):329-33.
7. Kaul DK, Thangaswamy S, Suzuka SM, Fabry ME, Wanderer AA, Gram H. Anti-Interleukin-1β Antibody-Based Therapy Ameliorates Endothelial Activation and Inflammation in Sickle Mice. Blood. 2011;118(21):388-.
8. Jang JE, Hidalgo A, Frenette PS. Intravenous immunoglobulins modulate neutrophil activation and vascular injury through FcgammaRIII and SHP-1. Circ Res. 2012;110(8):1057-66.
9. Nimmerjahn F, Ravetch JV. Fcgamma receptors as regulators of immune responses. Nat Rev Immunol. 2008;8(1):34-47.
10. Almeida CB, Souza LE, Leonardo FC, Costa FT, Werneck CC, Covas DT, et al. Acute hemolytic vascular inflammatory processes are prevented by nitric oxide replacement or a single dose of hydroxyurea. Blood. 2015;126(6):711-20.
11. Vandesompele J, De Preter K, Pattyn F, Poppe B, Van Roy N, De Paepe A, et al. Accurate normalization of real-time quantitative RT-PCR data by geometric averaging of multiple internal control genes. Genome Biol. 2002;3(7):RESEARCH0034.

Supplementary Table 1. Primers for quantitative Real-Time PCR

Gene	Protein encoded	Primer	Primer concentration
Actb - F *Actb - R*	β-Actin	5´- ACTGCCGCATCCTCTTCCT -3´ 5´- GAACCGCTCGTTGCCAATA- 3´	70nM
Gapdh - F *Gapdh-R*	GAPDH	5´- TGCACCACCAACTGCTTA -3´ 5´- GGATGCAGGGATGATGTTA -3	70nM
Col1a1- F *Col1a1- R*	Collagen Type 1	5´-GAGCGGAGAGTACTGGATCG -3´ 5´- GCTTCTTTTCCTTGGGGTTC- 3´	300nM
Col3a1 -F *Col3a1 -R*	Collagen Type 3	5´-GCACAGCAGTCCAACGTAGA- 3´ 5´- TCTCCAAATGGGATCTCTGG -3´	300 nM
Timp-1 -F *Timp-1 -R*	TIMP-1	5´- GCCTGTAGCTGTGCCCCA -3´ 5´- GGAACCCATGAATTTAGCCCTTAT	300nM
Timp-2 -F *Timp-2 -R*	TIMP-2	5´-GGGTCTCGCTGGACGTTG -3´ 5´- GGGTAATGTGCATCTTGCCAT -3´	300nM
Tgfb1– F *Tgfb1 - R*	TGF-β	5´- AAAGAAGTCACCCGCGTGC -3´ 5´- CCCGAATGTCTGACGTATTGAA -3´	300nM
Hif1a -F *Hif1a -R*	HIF-1α	5´-GAAGCACTAGACAAAGTTCACCTG-3´ 5´- TTAGGCTGGGAAAAGTTAGGAGT- 3´	150nM
Icam1 -F *Icam1 -R*	ICAM-1	5´- CAATTTCTCATGCCGCACAG -3´ 5´- AGCTGGAAGATCGAAAGTCCG -3´	70nM
Havcr1 -F *Havcr1 -R*	KIM-1	5´- GCATCTCTAAGCGTGGTTGC - 3´ 5´-TCAGCTCGGGAATGCACAA -3´	150nM
Lcn2 -F *Lcn2 -R*	NGAL/LCN2	5´- TGAAGGAACGTTTCACCCGCTTTG-3´ 5´- ACAGGAAAGATGGAGTGGCAGACA-3´	150nM
Tfrc -F *Tfrc -R*	TFR1	5´-AATGGTTCGTACAGCAGCGGAAG-3´ 5´- CACGAGCGGAATACAGCCACTG-3´	300nM
Hamp -F *Hamp -R*	Hepcidin	5´-CCTATCTCCATCAACAGATG- 3´ 5´- AACAGATACCACACTGGGAA-3´	300nM
Bmp6 – F *Bmp6 - R*	BMP6	5´- ATGGCAGGACTGGATCATTGC -3´ 5´- CCATCACAGTAGTTGGCAGCG-3´	70nM

GAPDH, glyceraldehyde-3-phosphate dehydrogenase; HIF-1α, Hypoxia-Inducible Factor 1α; ICAM-1, Intercellular adhesion molecule-1 (CD54); KIM-1, kidney injury molecule-1; LCN2/NGAL, neutrophil gelatinase-associated lipocalin; TIMP, Tissue inhibitor of metalloproteinases; TGF-β, Transforming Growth Factor-β.

Supplementary Table 2. Biochemical markers of organ damage in hemi- and homozygous SCD Berkeley mice treated or not with anti-CD62P and/ or anti-IL-1β therapy for 6 weeks

	N	AST (U/ML)[a]	ALT (U/ML)[a]	Total Bilirubin (mg/dL)[a]	Direct Bilirubin (mg/dL)[a]	Indirect Bilirubin (mg/dL)[a]	Creatinine (mg/dL)[b]
Hemizygous control	5	52.3±12.8	9.4±2.2	0.50±0.06	0.13±0.04	0.40±0.5	34.1±2.6
Homozygous SCD							
Saline	8	53.0±9.7	61.1±11.8 ###	1.30±0.2 ##	0.51±0.1 ###	0.92±0.09#	29.0±4.7
IgG1	8	53.5±6.2	68.8±14.5 ###	1.4±0.1 ##	0.52±0.1 ###	0.84±0.08#	24.2±2.3 #
Treatment							
Anti-CD62P	8	53.8±21.8	76.5±17.5	1.5±0.1	0.58±0.1	0.89±0.06	32.4±4.0
Anti-IL-1β	6	50.1±4.9	50.5±9.5	1.3±0.1	0.47±0.1	0.81±0.06	28.9±3.0
Anti-CD62P + anti-IL-1β	7	64.6±5.6	121.5±24.4$	1.5±0.1	0.40±0.06	1.10±0.09*$	31.5±9.9

[a] serum samples and [b] urine samples

Biochemical markers in the serum or urine of aged-matched hemizygous (SA) mice and homozygous (SS) Berkeley mice. Mice (4-months old) received administrations of *i.p.* saline (twice weekly) or *i.p.* injections of 30 µg/mouse IgG1 (three times a week) for six weeks, or were treated with i.p. injections of 30 µg/mouse anti-CD62P (three times a week), and /or 7.5 mg/Kg (twice a week) of anti-IL1β antibody for 6 weeks. Peripheral blood was obtained from animals at 48 hours after the last administration, before animal euthanasia. AST, aspartate aminotransferase; ALT, alanine aminotransferase. #, P<0.05; ##, p<0.01; ###, P<0.001 when compared to hemizygous (SA) mice. *, P<0.05 when compared to IgG1-control SS mice. $, P<0.05 when compared to Anti-IL-1β-treated SS mice.

Supplementary Table 3. Summary of the effects of mono- and combined immunotherapies.

	Vaso-occlusive Processes	Leukocyte-platelet aggregates		Leukocyte rolling	Leukocyte Adhesion	Inflammatory Markers	Biochemical markers	Liver injury	Liver vessel congestion	Liver macrophages	Iron deposition (liver/Kidney)
Anti-P-selectin	↓↓	↓↓	↓↓	↓↓	→	→ →	→	→	→	↓	→
Anti-IL-1β	↓↓	→	→	↓↓	↓↓	sICAM-1↓↓ TNF↓ IL-10 ↓↓ IL-6↓	→	↓↓	↓	↓↓	↓↓
Anti-P-selectin + Anti-IL-1β	↓↓	↓↓	↓↓	↓↓	↓↓	TNF↓	↑ALT, IB	↑*	↓	↓	↓↓

Acute administration effects; Long-term administration effects; → no significant effect; ↓ decrease ($p<0.05$); ↓↓ decrease ($p<0.01$); ↑ increase.

* Histopathological features. ALT, alanine aminotransferase; IB, indirect bilirubin

Supplementary Figures

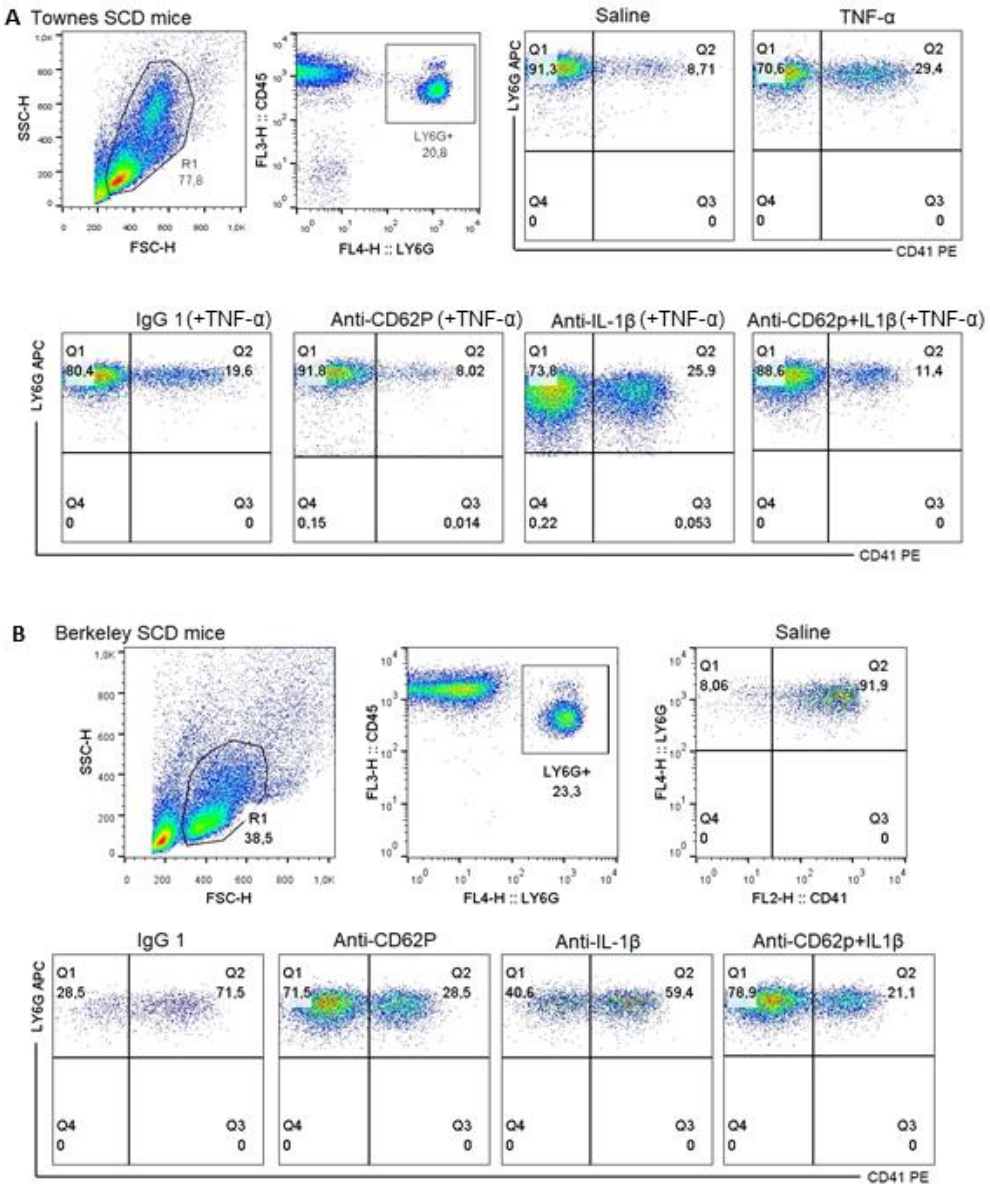

Supplementary Figure 1. Flow cytometry-gating strategy for analysis, and representative dot plots, for neutrophil-platelet aggregates in blood samples from **(A)** Townes mice, and **(B)** Berkeley mice. Peripheral blood was obtained from the retro-orbital plexus of mice and incubated with PerCP anti-mouse CD45, APC anti-mouse Ly6G, and PE anti-mouse CD41, before lysing red blood cells. Data acquisition (50,000 events) was performed on a FACSCalibur™ Flow Cytometer. $CD45^{+}Ly6G^{+}$ neutrophils were gated, and those that also labelled positive for CD41 were considered to be neutrophil-platelet aggregates (calculated using FlowJo V10 analysis software).

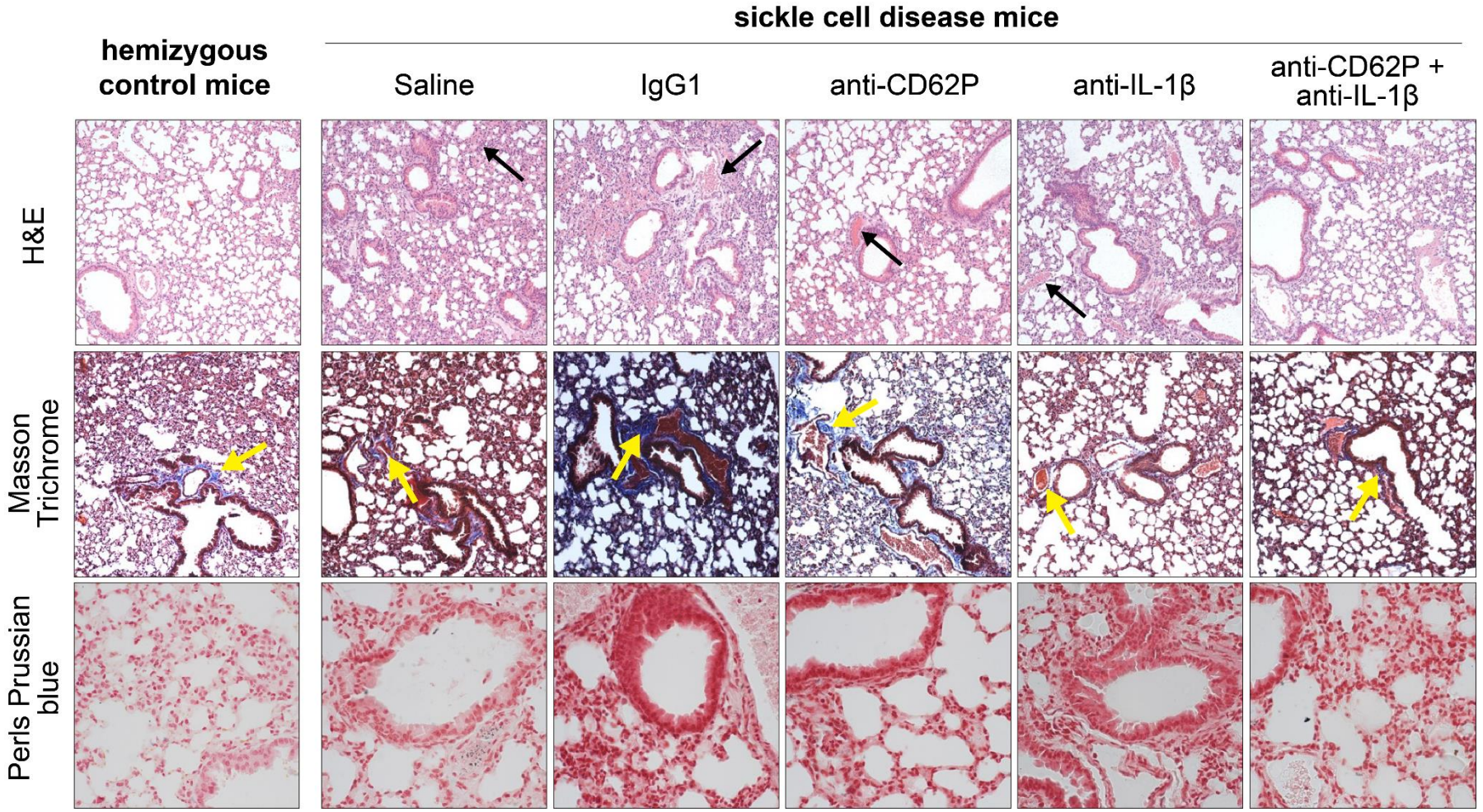

Supplementary Figure 2: Effects of 6-weeks administration of anti-CD62P and anti-IL-1β immunotherapies on lung histology, injury, and iron accumulation in sickle cell disease mice. Berkeley SCD mice (4-months old) were treated, or not, with immunotherapies for 6 weeks. At 48 h after administration of the final intervention dose, lungs were dissected and processed for histological analysis (H & E staining, 20x magnification), analysis of fibrosis (Masson Trichrome, 20x mag.), iron accumulation (Perls Prussian blue, 63x mag.). Representative photographs of stained paraffin-embedded sections from each treatment group and comparison with lung sections from hemizygous Berkeley control mice of the same age. Photographs are representative of four images per section (2-4 sections/mouse). Black arrows: congested vessels; yellow arrows: collagen deposits. Photomicrographs taken with a Zeiss Axio Imager D2.

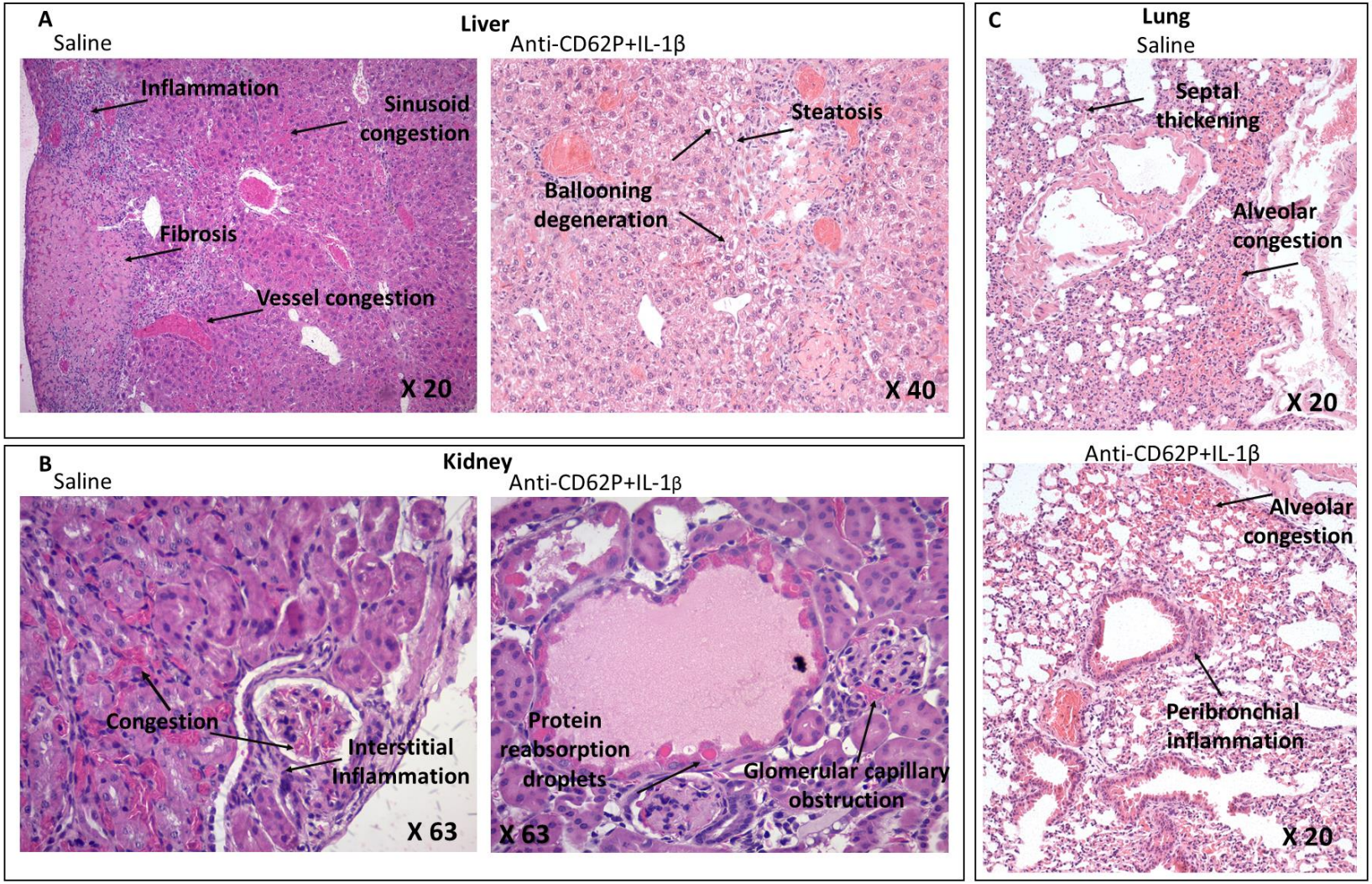

Supplementary Figure 3: Representative histopathological features (H&E staining) observed in the (A) liver, (B) kidney and (C) lung of SCD mice following 6 weeks of administration of saline, or of anti-CD62P and anti-IL-1β combined therapy. Photomicrographs taken with a Nikon microscope, model BM2100.

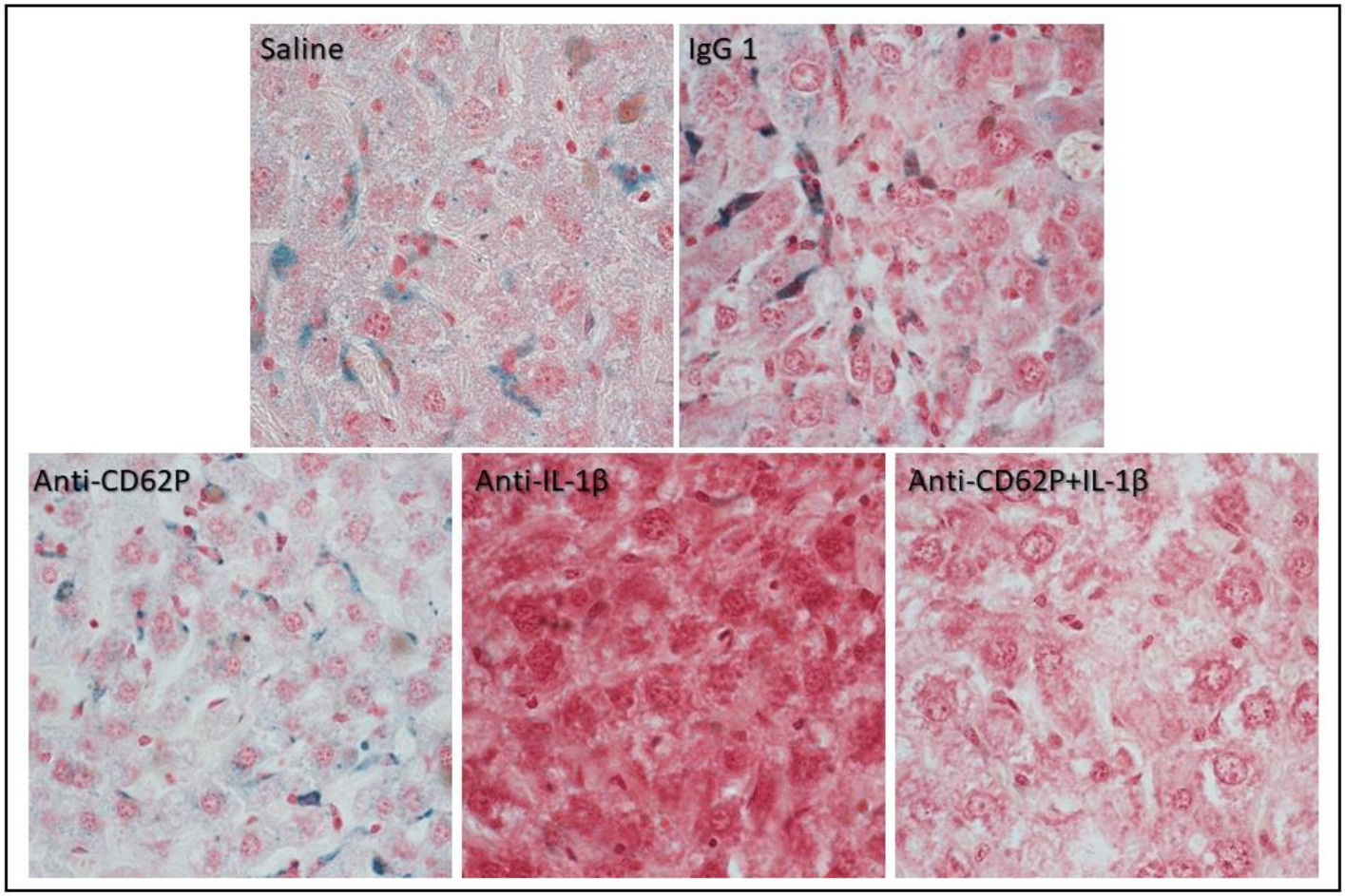

Supplementary Figure 4. Representative high magnification photomicrographs of iron deposition (blue staining) associated with macrophage infiltration in liver sections of Berkeley SCD mice (22 weeks old) after 6 weeks of the indicated administration. Perls staining; livers from anti-IL-1β and anti-CD62P + IL-1β-treated mice did not present iron deposition. Images (X100) were taken with a Zeiss Axio Imager D2.

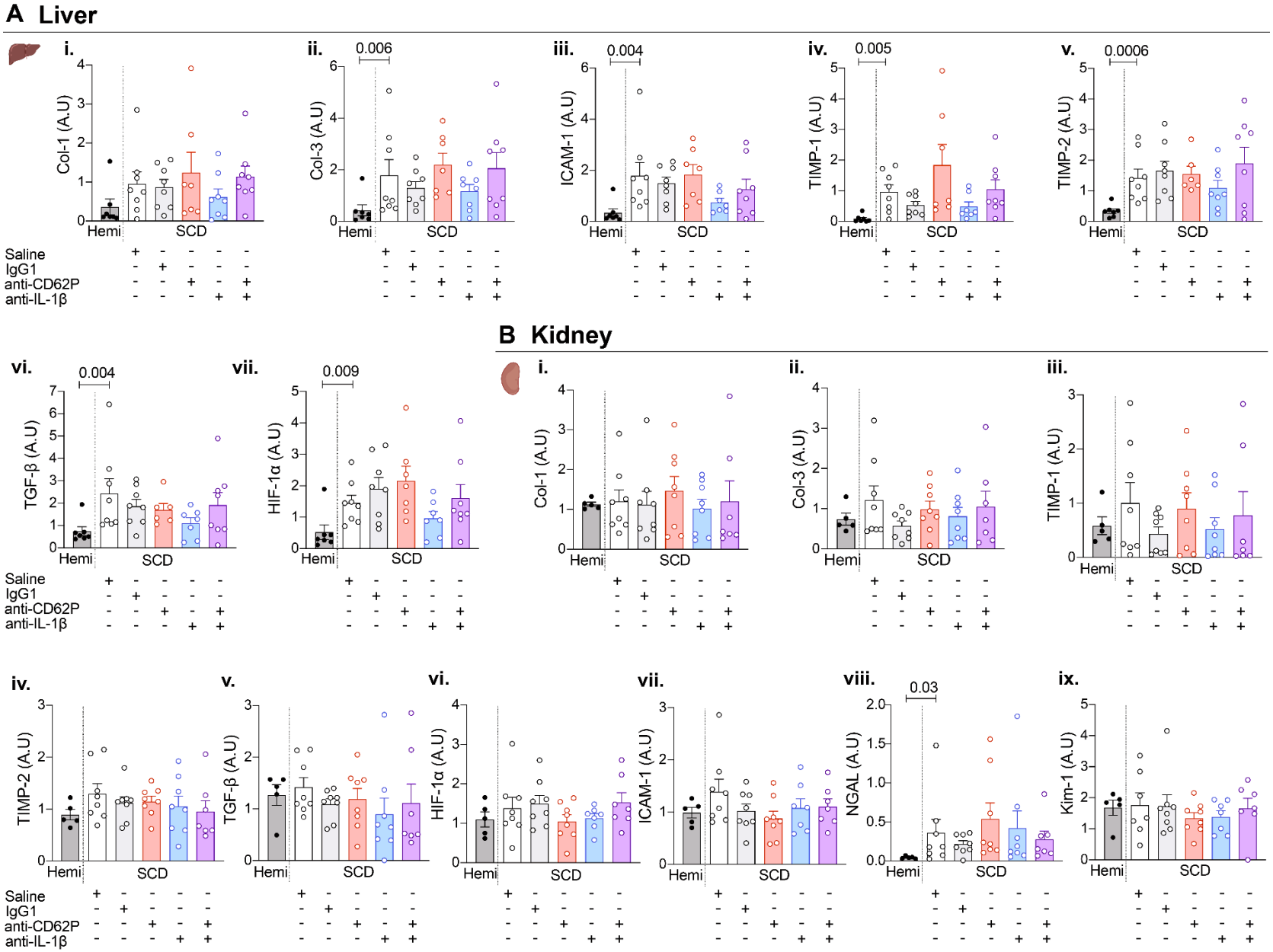

Supplementary Figure 5. Gene expressions of biomarkers of inflammation and damage in organs of aged-matched hemizygous and homozygous Berkeley SCD mice following treatment for 6 weeks, according to Figure 3A. (A) Liver, and (B) kidney. Genes and their encoded proteins are described in the Supplementary Table 1; expressions were quantified by qPCR.